Contribution of hydroxymethanesulfonate (HMS) to severe winter haze in the North China Plain

Tao Ma[1], Hiroshi Furutani[2,3], Fengkui Duan[1], Takashi Kimoto[4], Jingkun Jiang[1], Qiang Zhang[5], Xiaobin Xu[6], Ying Wang[6], Jian Gao[7], Guannan Geng[1], Meng Li[5], Shaojie Song[8], Yongliang Ma[1], Fei Che[7], Jie Wang[7], Lidan Zhu[1], Tao Huang[4], Michisato Toyoda[3], Kebin He[1]

[1]State Key Joint Laboratory of Environment Simulation and Pollution Control, School of Environment, State Environmental Protection Key Laboratory of Sources and Control of Air Pollution Complex, Beijing Key Laboratory of Indoor Air Quality Evaluation and Control, Tsinghua University, Beijing 100084, China
[2]Support Center for Scientific Instrument Renovation and Custom Fabrication, Osaka University, Osaka, 560-0043, Japan
[3]Project Research Center for Fundamental Sciences, Graduate School of Science, Osaka University, Osaka, 560-0043, Japan
[4]Kimoto Electric Co., Ltd, 3-1 Funahashi-cho Tennoji-ku, Osaka 543-0024, Japan
[5]Ministry of Education Key Laboratory for Earth System Modeling, Department of Earth System Science, Tsinghua University, Beijing 100084, China
[6]State Key Laboratory of Severe Weather & Key Laboratory for Atmospheric Chemistry of CMA, Chinese Academy of Meteorological Sciences, Beijing 100081, China
[7]State Key Laboratory of Environmental Criteria and Risk Assessment, Chinese Research Academy of Environmental Sciences, Beijing 100012, China
[8]School of Engineering and Applied Sciences, Harvard University, Cambridge, MA 02138, USA

Correspondence to: Fengkui Duan (duanfk@mail.tsinghua.edu.cn) and Kebin He (hekb@tsinghua.edu.cn)

Abstract. Severe winter haze accompanied by high concentrations of fine particulate matter ($PM_{2.5}$) occurs frequently in the North China Plain and threatens public health. Organic matter (OM) and sulfate are recognized as major components of $PM_{2.5}$, while atmospheric models often fail to predict their high concentrations during severe winter haze due to incomplete understanding of secondary aerosol formation mechanisms. By using a novel combination of single particle mass spectrometry and an optimized ion chromatography method, here we show that hydroxymethanesulfonate (HMS), formed by the reaction between formaldehyde (HCHO) and dissolved SO_2 in aerosol water, is ubiquitous in Beijing during winter. The HMS concentration and the molar ratio of HMS to sulfate increased with the deterioration of winter haze. High concentrations of precursors (SO_2 and HCHO) coupled with low oxidant levels, low temperature, high relative humidity, and moderately acidic pH facilitate the heterogeneous formation of HMS, which could account for up to 15% of OM in winter haze and lead to up to 36% overestimates of sulfate when using traditional ion chromatography. Despite the clean air actions have substantially reduced SO_2 emissions, the HMS concentration and molar ratio of HMS to sulfate during severe winter haze increased from 2015 to 2016 with the growth of HCHO concentration. Our findings illustrate the significant contribution of heterogeneous HMS chemistry to severe winter haze in Beijing, which help to improve the prediction of OM and sulfate, and suggest that the reduction in HCHO can help to mitigate haze pollution.

1 Introduction

35   Severe winter haze pollution with high PM$_{2.5}$ (particles with aerodynamic diameter ≤ 2.5 μm) concentration occurs frequently in the North China Plain (NCP), exerting adverse impacts on the environment and human health (Huang et al., 2014; Lelieveld et al., 2015). Secondary components, constituting a large fraction of PM$_{2.5}$, are key drivers of haze formation (Huang et al., 2014), however, atmospheric models with known formation mechanisms often fail to predict high levels of secondary organic matter (OM) and sulfate during severe winter haze.

40   Traditional models with gas-phase photochemical mechanisms and aqueous chemistry involving glyoxal and methylglyoxal significantly underestimate the high OM levels observed in the NCP during winter (Wang et al., 2014; Zheng et al., 2015a). Adding heterogeneous reactions involving isoprene epoxide, glyoxal, and methylglyoxal, and accounting for organic aerosol aging and oxidation of intermediate-volatility organic compounds can improve the model predictions of OM (Zhao et al., 2016; Hu et al., 2017; Yang et al., 2018), however, high OM concentrations observed in Beijing winter are still underpredicted (Hu

45   et al., 2017), especially during the periods with low oxidant concentrations and weak photochemical activity.

In addition to OM, high levels of particulate sulfate are often observed in the NCP during winter, which increase sharply with increasing PM$_{2.5}$ pollution levels (Zheng et al., 2015b). Traditional atmospheric models containing both gas-phase oxidation of SO$_2$ by OH radicals and aqueous-phase reaction pathways involving H$_2$O$_2$, O$_3$, and O$_2$ catalyzed by Fe^{3+} and Mn^{2+} fail to reproduce the observed high sulfate levels, and revised models with heterogeneous chemistry greatly improve the sulfate

50   simulation (Wang et al., 2014; Zheng et al., 2015a). Cheng et al. (2016) and Wang et al. (2016) reported that the oxidation of SO$_2$ by NO$_2$ in aerosol water under high pH could explain the difference between modeled and observed sulfate. On the other hand, the misidentification of organosulfur compounds as inorganic sulfate in conventional measurements can lead to overestimation of the observed particulate sulfate (Chen et al., 2019). Recently, Moch et al. (2018) and Song et al. (2019) reported the potential contribution of hydroxymethanesulfonate (HMS, HOCH$_2$SO$_3^-$) to particulate sulfur during winter haze

55   in Beijing. However, there is no direct observational evidence for the presence of HMS in haze particles, and the formation mechanism of HMS in NCP winter haze is still unclear.

HMS was previously found at appreciable concentrations in cloud and fog (Munger et al., 1986; Rao and Collett, 1995), whereas the HMS concentrations observed in atmospheric aerosols in the United States, Germany, and Japan were low (Dixon and Aasen, 1999; Suzuki et al., 2001; Scheinhardt et al., 2014). If HMS does play a role in NCP winter haze, unambiguous

60   identification and accurate quantification of aerosol HMS are essential. Low oxidant concentrations, high water content, moderate pH, and low temperatures for typical cloud and fog conditions together with the presence of SO$_2$ and formaldehyde (HCHO) favor HMS formation (Boyce and Hoffmann, 1984; Deister et al., 1986; Kok et al., 1986; Lagrange et al., 1999). Such conditions are common during severe winter haze in the NCP, such as Beijing (Zheng et al., 2015b; Cheng et al., 2016; Rao et al., 2016).

65   In this study, combining aerosol time-of-flight mass spectrometry (ATOFMS) measurement and an optimized ion chromatography method, we identified the ubiquity of HMS in Beijing during winter and quantified its contribution to severe

winter haze. We demonstrate that the reaction between HCHO and dissolved SO_2 to form HMS in aerosol water is an important pathway that contributes to winter haze pollution in Beijing, not only accounting for a substantial mass of OM but also leading to overestimation of sulfate in conventional measurements. High concentrations of precursors (i.e., SO_2 and HCHO) coupled with appropriate conditions (i.e., low oxidants, low temperature, high relative humidity, and moderately acidic pH) in severe winter haze favor heterogeneous HMS formation. Furthermore, two-year continuous winter measurements from 2015 to 2016 indicate that HMS concentrations increased with the increase of HCHO. Finally, we discuss the implications of heterogeneous HMS chemistry for haze chemistry and control strategies.

2 Methods

2.1 Sampling site

Field measurements were conducted in urban Beijing in the winter of 2015 and 2016. The observational sites are located at Tsinghua University (40.00° N, 116.34° E), the Chinese Academy of Meteorological Sciences (39.95° N, 116.33° E), and the Chinese Research Academy of Environmental Sciences (40.05° N, 116.42° E), respectively (Fig. S1 in the Supplement). Details of the measurements and analysis are described below.

2.2 ATOFMS measurement and data analysis

Real-time ATOFMS (model 3800-100, TSI, Inc.) measurement in Beijing was carried out from December 21, 2015 to January 8, 2016. The observation site was on the tenth floor of the School of Environment, Tsinghua University, approximately 35 m above ground level. Details of ATOFMS measurements have been described in previous studies (Furutani et al., 2011). Briefly, ATOFMS simultaneously measures the size and chemical composition of individual particles. The inlet flow rate is $0.1 \, L \, min^{-1}$. Ambient aerosols between 100 nm and 3000 nm enter the ATOFMS instrument through an aerodynamic focusing lens and are accelerated to their size-dependent terminal velocities. The particle velocity is determined by measuring the time-of-flight between two solid state green lasers ($\lambda = 532$ nm, 50 mW, CL532‑050‑L, CrystaLaser, NV, USA). The particle size is calculated from the measured velocity based on the calibration curve between particle size and velocity. In addition, the velocity is used to trigger the 266 nm Nd:YAG laser (~1 mJ/pulse), which desorbs and ionizes the particle. The generated positive and negative ions are detected using a bipolar reflectron time-of-flight mass analyzer. The ATOFMS aerodynamic sizing was calibrated by standard polystyrene latex spheres (PSL) with different sizes (d = 151, 199, 269, 350, 499, and 799 nm, Duke Scientific Corp., USA). Mass calibration of the ATOFMS instrument was conducted with the standard solution (Ba, K, Pb, Na, Li, V in HNO_3).

During the winter campaign, ATOFMS detected 4,495,233 particles containing both size and chemical information, accounting for 49% of all sized particles. Single particle mass spectrometers identify the peak at m/z 111 in the negative ion mode as HMS (Neubauer et al., 1997; Whiteaker and Prather, 2003; Dall'Osto et al., 2009). To eliminate interferences, HMS-containing

particles were screened with a relatively high threshold: the peak area at *m/z* 111 in the negative ion mode should be greater than 2% of the total integrated area of the single particle negative ion mass spectrum (Whiteaker and Prather, 2003).

2.3 Offline sample collection and ion chromatography analysis

PM$_{2.5}$ samples were collected on 47 mm quartz filters at a flow rate of 15.4 L min^{-1} for 23.5 hours every day. Here, we analyzed 36 and 33 samples in the winter of 2015 and 2016, respectively. In the winter of 2016, we also collected 3 and 5 PM$_{2.5}$ samples on 90 mm quartz filters at a flow rate of 100 L min^{-1} in the day- and nighttime, respectively. The filters were baked in a Muffle furnace at 550°C for 4 h, put in the cassettes, and packed using aluminum foil prior to sampling, and all samples were stored at −20°C before analysis. A quarter of each 47 mm filter or 3.14 cm^2 punch from each 90 mm filter was extracted twice with 5 mL 0.1% HCHO solution, ultrasonic agitation for 20 min in an ice water bath and then filtered through the 0.45 μm membrane syringe filter. Two extracts were combined for ion chromatography analysis. We found that HMS slowly converted to sulfate during conventional sample preparation (i.e. water extraction), leading to HMS underestimation and sulfate overestimation, whereas extraction with 0.1% HCHO solution can counteract the HMS decomposition (Fig. S2a, b).

A Dionex Integrion HPIC Ion Chromatography system with AS11-HC analytical column and AG11-HC guard column (Dionex Corp., CA, US), typical columns used in previous studies during winter haze in Beijing (Cao et al., 2014), was used for the anion analysis. The separation of HMS and sulfate depends on ion chromatography conditions (i.e., column and eluent). We found the separation of HMS and sulfate peak was not complete under conventional conditions (eluent: 30 mM KOH, flow rate: 1.5 mL min^{-1}) (Fig. S2c). Here, we used an eluent of 11 mM KOH (pH≈12) with a flow rate 1.5 mL min^{-1}, and successfully distinguished HMS from sulfate (Fig. S2d). In addition, Moch et al. (2018) and Dovrou et al. (2019) found that the AS22 column could not fully separate HMS and sulfate, while AS12A was able to successfully separate HMS and sulfate. HMS dissociates into SO$_3^{2-}$ and HCHO rapidly in the eluent due to the short characteristic time for HMS dissociation at pH 12, and the HMS concentration is measured in the form of sulfite in ion chromatography (Fig. S2e) (Dasgupta, 1982). Thus, the ion chromatography method cannot distinguish HMS from sulfite directly. Previous studies indicated that the concentration of sulfite in atmospheric aerosols was much lower than that of HMS (Dixon and Aasen, 1999; Dabek-Zlotorzynska et al., 2002). In order to distinguish between sulfite and HMS, a second analysis was performed using dilute nitric acid (pH≈3) to extract samples. In the second analysis, sulfite is oxidized to sulfate, while HMS is stable. We tested some samples collected during severe winter haze in Beijing, and found that the influence of sulfite on HMS measurement was negligible (Fig. S2f). The method detection limit was 0.02 mg L^{-1} for SO$_3^{2-}$, equal to 0.03 mg L^{-1} for HMS. The blank quartz filter was analyzed as control. We also tested the accuracy (through recovery analysis) and precision (through repetitive analysis) of the method on HMS analysis. The recovery of blank and sample was 95.6% and 112.5%, respectively. The relative standard deviation (RSD) of triple repetitive analysis of the sample (average: 3.17 mg L^{-1}) was 4.7%.

2.4 Supplementary data and analysis

Online measurements of gaseous pollutants, particulate matter, and meteorological parameters were conducted on the roof of

School of Economics and Management, approximately 20 m above ground level and 100 m away from the ATOFMS observation site, on the campus of Tsinghua University as described in previous works (Zheng et al., 2015b; Xu et al., 2017). In brief, hourly mass concentrations of $PM_{2.5}$ and PM_1 were monitored based on the β-ray absorption method by using two dichotomous monitors (PM-712 and PM-714; Kimoto Electric Co., Ltd., Japan). The hourly concentrations of carbonaceous species including organic carbon (OC) and elemental carbon (EC) in $PM_{2.5}$ in 2015 winter were monitored by APC-710 (Kimoto Electric Co., Ltd., Japan). The hourly OC and EC concentrations in $PM_{2.5}$ in 2016 winter were measured by a Sunset Model 4 Semi-Continuous Carbon Analyzer (Beaverton, OR, USA). We adopted a factor of 1.6 to convert the OC mass into OM mass (Xing et al., 2013; Zhang et al., 2017). The hourly concentrations of gaseous pollutants including SO_2, CO, and O_3 were monitored with MCSAM-13 system (Kimoto Electric, Ltd., Japan). The hourly meteorological parameters including temperature and relative humidity (RH) were simultaneously monitored with an automatic meteorological observation instrument (Milos 520, VAISALA Inc., Finland).

Online concentrations of water-soluble ions in $PM_{2.5}$ and inorganic gases were measured by a Monitor for AeRosols and GAses (MARGA, Metrohm Ltd., Switzerland) in 2016 winter at the Chinese Research Academy of Environmental Sciences, about 9 kilometers from Tsinghua University. We calculated the aerosol water content and pH with the ISORROPIA-II thermodynamic equilibrium model (Fountoukis and Nenes, 2007). Briefly, we adopted the forward mode constrained by gas (HNO_3, HCl, and NH_3) + aerosol (SO_4^{2-}, NO_3^-, Cl^-, K^+, Ca^{2+}, Na^+, Mg^{2+}, NH_4^+) measurements, and assumed the aerosol phase state to be metastable (Hennigan et al., 2015). The model inputs were taken from the MARGA measurements.

Online HCHO measurement was conducted in 2015 winter at the Chinese Academy of Meteorological Sciences, about 6 kilometers from Tsinghua University. Ambient HCHO was measured by an Aero-Laser GmbH HCHO analyzer (model AL4021) based on the Hantzsch reaction, as described in previous work (Song et al., 2019). The Hantzsch reagents were prepared every 3 days and stored in a refrigerator. This analyzer was calibrated with a 1 μM HCHO standard solution every 2 to 3 days. The detection limit is 150 ppt in the field, and the accuracy and precision are ±15% or 150 ppt and ±10% or 150 ppt, respectively (Hak et al., 2005).

The anthropogenic emission inventory data of HCHO was derived from the Multi-resolution Emission Inventory of China (MEIC) model framework (available at http://www.meicmodel.org/), as described in detail in earlier papers (Li et al., 2019b). Briefly, the emissions were calculated based on a technology-based methodology using updated activity data from the MEIC model framework and a collection of state-of-the-art emission factors and source profiles. The uncertainty of volatile organic compounds (VOCs) emission inventory in MEIC was estimated to be ±68% (Cheng et al., 2019).

3 Results and discussion

3.1 Identification of HMS in atmospheric particles

Our field measurements with ATOFMS showed that HMS was ubiquitous in aerosols from Beijing during winter. We found that 76% of particles contained the peak at *m/z* 111 in the negative ion mode, and screened HMS-containing particles (the

relative peak area at m/z 111 in the negative ion mode greater than 2%, Fig. 1) accounted for 9% of the total particles. It should be noted that KCl_2^- and methyl sulfate ($CH_3SO_4^-$) could also contribute to the peak at m/z 111 in the negative ion mode. According to the natural isotopic distribution, the contribution of KCl_2^- was found to be insignificant. The peak area ratio of m/z 111 to m/z 113 in the negative ion mode in all screened particles was 18.7, which was consistent with the natural isotopic distribution of HMS (18.7) and much larger than that of KCl_2^- (4.8). Also, the peak area ratio of m/z 109 to m/z 111 in the negative ion mode in all screened particles was 0.03, which was much smaller than that of KCl_2^- (1.4). Considering the moderate aerosol pH (4–5; see Sect. 3.3) in Beijing winter haze and the tendency of m/z 111 in the negative ion mode to exist in supermicrometer particles (see Sect. 3.2) in this study, the peak at m/z 111 in the negative ion mode unlikely corresponds to methyl sulfate since methyl sulfate formation requires relatively high acidic conditions (Lee, 2003) and organosulfates tend to exist in submicrometer particles (Hatch et al., 2011). Therefore, the peak at m/z 111 in the negative ion mode in ambient particles can safely be assigned to HMS. Ambient particles in Beijing during winter contained a large amount of ammonium relative to sodium, and the ammonium was more common than sodium in HMS-containing particles (Fig. S3), indicating that the matrix effects on HMS detection due to counterions was not significant, because ammonium promotes the presence of the HMS marker peak in the negative ion spectrum (Neubauer et al., 1997; Whiteaker and Prather, 2003). The mass spectrum of HMS-containing particles observed in this study is similar to previous studies (Whiteaker and Prather, 2003; Dall'Osto et al., 2009; Song et al., 2019). In general, the positive mass spectra are characterized by the presence of ammonium (m/z 18 NH_4^+), elemental carbon (m/z 12 C^+, 36 C_3^+, 48 C_4^+, and 60 C_5^+), and organic carbon (m/z 27 $C_2H_3^+$, 37 C_3H^+, 39 $C_3H_3^+$, and 43 $C_2H_3O^+$), whilst the peaks at m/z 46 (NO_2^-), 62 (NO_3^-), 80 (SO_3^-), 81 (HSO_3^-), and 97 (HSO_4^-) are common in the negative mass spectra.

3.2 Quantification of HMS in atmospheric particles

Based on the optimized ion chromatography method, we determined the HMS concentration and its contribution to haze pollution in winter. We found that the HMS concentration was appreciable in humid haze conditions, but low in clean and dry haze conditions (Fig. S4). The HMS concentration exhibited similar periodic variation to that of $PM_{2.5}$ and sulfate concentration in winter, and was consistent with the variation of RH. With the deterioration of winter haze in 2015, i.e., from clean ($PM_{2.5} \leq$ 75 μg m^{-3}, 10 days), polluted ($75 < PM_{2.5} \leq 150$ μg m^{-3}, 12 days) to heavily polluted ($PM_{2.5} > 150$ μg m^{-3}, 14 days), the HMS concentration increased rapidly (Fig. 2a). Also, the molar ratio of HMS to sulfate increased from 0 (clean), 0.02 (polluted), to 0.06 (heavily polluted). During the HMS increase process, RH, SO_2, and the HCHO concentration increased, while the O_3 concentration declined (Fig. 2b, c). HMS tends to exist in supermicrometer particles. During the HMS events, the ratio of $PM_{1-2.5}$ to $PM_{2.5}$ was generally greater than 0.4, indicating a large contribution of supermicrometer aerosols. The size distribution of HMS-containing particles displayed a mode at larger sizes compared with the total particle size distribution, and the percentage of HMS-containing particles increased with particle size and remained relatively constant when the diameter is greater than 1 μm (Fig. 2d), indicating the predominance of HMS in larger particles.

Field measurements in Beijing in winter 2016 showed a similar HMS evolution as that of winter 2015, i.e., high HMS

concentrations usually occurred in humid haze conditions with high concentrations of precursors, high RH, and weak photochemical activity (Fig. S5 and S6), but HMS concentrations were higher than in winter 2015. During severe winter haze ($PM_{2.5}$ > 150 μg m^{-3}), the concentrations of HMS, $PM_{2.5}$, OM, and sulfate were 4 μg m^{-3} (0.7–9.6 μg m^{-3}), 224 μg m^{-3} (160–379 μg m^{-3}), 83 μg m^{-3} (45–121 μg m^{-3}), 45 μg m^{-3} (23–108 μg m^{-3}) and 7 μg m^{-3} (0.4–18.5 μg m^{-3}), 237 μg m^{-3} (154–339 μg m^{-3}), 97 μg m^{-3} (65–147 μg m^{-3}), 36 μg m^{-3} (15–66 μg m^{-3}) in 2015 and 2016, respectively. The HMS accounted for 1.5% (0.4–4%) of $PM_{2.5}$ mass in 2015, and this contribution increased to 2.7% (0.3–6%) in 2016 (Fig. S7). Correspondingly, the contribution of HMS to estimated OM increased from 4.4% (0.9–11%) in 2015 to 7.6% (1.4–15%) in 2016. The increase of HMS from winter 2015 to winter 2016 was consistent with the increasing HCHO concentration. Instead, the concentrations of SO_2 during severe winter haze decreased significantly due to the strict control measures, resulting in a decrease of sulfate. Accordingly, the molar ratio of HMS to sulfate increased significantly from winter 2015 to winter 2016. Considering the conversion of HMS to sulfate in conventional ion chromatography analysis, the observed sulfate concentrations during severe winter haze could be overestimated by 6.4% (3–15%) in 2015, and the ratio increased to 15% (2.5–36%) in 2016.

3.3 Factors influencing HMS formation

HMS is formed in the aqueous phase, such as cloud (Moch et al., 2018), fog (Munger et al., 1986), and aerosol water (Song et al., 2019). We find that HMS is present in aerosols regardless of the presence of cloud/fog (Fig. S8a, b), and HMS concentrations show a good correlation (r = 0.92, P < 0.01) with aerosol water content (Fig. S8b), indicating that aerosol water serves as a medium for HMS formation. In some HMS events, cloud/fog processes exist (Fig. S8a, b) and may contribute together with heterogeneous processes in aerosol water to the formation of HMS. Our results indicate that high concentrations of precursors (i.e., SO_2 and HCHO) coupled with appropriate conditions (i.e., low oxidants, low temperature, high RH, and moderately acidic pH) in severe winter haze in the NCP facilitate the heterogeneous HMS formation.

Low oxidants and low temperature during winter haze facilitate the HMS formation. S(IV) oxidation reactions compete with HMS formation (Pandis and Seinfeld, 1989). The low O_3 concentration and low solar radiation during HMS events (Fig. S4 and S5) indicate the weak photochemical activity. Previous measurements also showed that OH radical and H_2O_2 concentrations were low in winter, especially during severe winter haze (Zhang et al., 2012; Tan et al., 2018; Ye et al., 2018). Low temperature increases the solubility of gas (Sander, 2015), whereas it decreases the reaction rate constant for HMS production (Boyce and Hoffmann, 1984). According to the kinetics calculation (Song et al., 2019), the increase of gas solubility in water at low temperature is greater than the decrease of the reaction rate constant, leading to higher HMS formation rate in winter haze. Once formed, HMS is relatively stable due to the self-acidification and resistance to oxidation by O_3, H_2O_2, and O_2 (Dasgupta et al., 1980; Hoigne et al., 1985; Kok et al., 1986; Munger et al., 1986).

High RH is a key factor driving fast HMS formation in winter haze. The HMS concentration increases slowly under low RH, whereas it increases rapidly under high RH (Fig. S9). Similarly, the aerosol water content exhibits an exponential increase with RH (Fig. S10), providing abundant reaction interfaces for HMS formation. The HMS concentration started to increase significantly with the enhancement in RH when the RH > 60%, coinciding with the reported deliquesce RH of particles in

Beijing winter (Liu et al., 2017b). With the increase of RH, the atmospheric sulfur distribution shifts toward the particle phase and more particulate sulfur exists in the form of HMS (Fig. 3). The molar ratio of HMS to sulfate also started to increase rapidly at the RH ~60%, and high values usually occurred under severe winter haze with high $PM_{2.5}$ and HMS concentrations.

230   Moderately acidic pH in Beijing winter haze favors the HMS formation. Previous studies indicated that both HMS formation and decomposition rate increased rapidly with pH, thereby high HMS concentrations were usually observed in moderate pH conditions, since low pH retards the formation of HMS, while high pH is not suitable for its preservation (Munger et al., 1986). The calculations based on the ISORROPIA-II thermodynamic equilibrium model constrained by in situ gas and aerosol measurements showed an average pH value of 4.5 (from 4 to 5) for aerosol water under severe winter haze in 2016, which

235   agreed reasonably with previous studies in the NCP (Liu et al., 2017a; Song et al., 2018; Ding et al., 2019; Ge et al., 2019; Li et al., 2019a) and was higher than those in the United States and Europe (Bougiatioti et al., 2016; Weber et al., 2016). Under such conditions, HMS formation is favored, whereas decomposition of HMS is negligible, thereby resulting in the observed high HMS concentrations during severe winter haze.

3.4 Implications for haze chemistry and control strategies

240   Our findings reveal the significant contribution of HMS to severe winter haze. We propose a more comprehensive conceptual model of heterogeneous sulfur chemistry in NCP haze events, including traditional sulfate formation, and HMS formation under high HCHO concentrations, low oxidant levels, low temperature, high RH, and moderate pH (Fig. 4a). With the deterioration of winter haze, the atmospheric oxidation capacity decreases with the weak photochemical activity, while heterogeneous HMS chemistry is enhanced, resulting in the increase of HMS concentration and the ratio of HMS to sulfate

245   (Fig. 4b). Adding heterogeneous HMS chemistry into the model could improve the simulation of OM. In addition, the presence of HMS could lead to sulfate overestimation in conventional measurements, such as ion chromatography and aerosol mass spectrometry (Song et al., 2019). This can partly explain the discrepancy between sulfate simulation and observation during severe NCP winter haze. Furthermore, HMS can be used as a tracer for heterogeneous chemistry and moderate pH during typical winter haze pollution.

250   Our results suggest that the reduction in HCHO concentration can help to mitigate severe winter haze pollution in the NCP. Previous studies show that HCHO is an important source of RO_x ($OH+HO_2+RO_2$) radicals and ozone (Niu et al., 2016; Tan et al., 2018; Li et al., 2019b), and has high toxicity as a Group 1 human carcinogen (Niu et al., 2016); in this study, we further demonstrate its significant contribution to particulate matter in winter. Since the implementation of 'Air Pollution Prevention and Control Action Plan' in 2013, SO_2 concentrations during winter haze in Beijing have decreased significantly due to the

255   implementation of desulfurization measures and controls on emission activities (Zheng et al., 2015b; Zheng et al., 2018), resulting in the decrease of sulfate, while HCHO concentrations show an increasing trend (Fig. S7), leading to the increased importance of HMS in winter haze. HCHO comes from primary emissions and secondary formation (Chen et al., 2014; Sheng et al., 2018). Therefore, the cooperative emission reduction in primary HCHO, which mainly comes from residential solid fuel (biofuel and coal) combustion and transportation (Fig. S11) (Li et al., 2019b), and VOCs (e.g., alkenes, aromatics, and alkanes)

260 related to secondary HCHO formation, should be considered in future pollutant control strategies in the NCP. Furthermore, the HMS chemistry and related control strategies can be applicable to other regions with high SO_2 and HCHO concentrations, such as India (De Smedt et al., 2015; Li et al., 2017).

4 Conclusion

Combining field measurements and laboratory experiments, we show the ubiquity of HMS in aerosols and the quantification
265 of the large amounts of HMS in $PM_{2.5}$ in Beijing during winter, and elucidate the heterogeneous HMS chemistry in winter haze. High concentrations of precursors (SO_2 and HCHO), low oxidant levels, low temperature, high RH, and moderately acidic pH during severe winter haze facilitate the heterogeneous formation of HMS, which could account for up to 15% of OM in winter haze and lead to up to 36% overestimates of sulfate. The HMS concentration and the molar ratio of HMS to sulfate increased with the deterioration of winter haze, as well as from winter 2015 to winter 2016 with the growth of HCHO
270 concentration. Our results reveal the significant contribution of HMS to severe winter haze, which help to improve the prediction of OM and sulfate, and suggest that the reduction in HCHO can help to mitigate severe winter haze pollution.

Data availability. All data that support the findings of this study are available in this article and its Supplement or from the corresponding author on request.

275 *Author contributions.* TM, FD, and KH designed research; TM, HF, FD, TK, JJ, YM, LZ, TH, MT, and KH performed research; TM, HF, TK, and SS contributed new reagents/analytic tools; TM and HF analyzed data; QZ, GG, and ML provided emission inventory; XX and YW provided formaldehyde data; JG and JW provided MARGA data; TM wrote the paper; and TM, HF, FD, JJ, QZ, and KH revised the paper.

Competing interests. The authors declare that they have no conflict of interest.

280 *Acknowledgements.* This work was supported by the National Science and Technology Program of China (2017YFC0211601), the National Natural Science Foundation of China (81571130090), and National Research Program for Key Issues in Air Pollution Control (DQGG0103). We thank Weiya Yu and Xiaodong Liu for helpful discussions.

References

Bougiatioti, A., Nikolaou, P., Stavroulas, I., Kouvarakis, G., Weber, R., Nenes, A., Kanakidou, M., and Mihalopoulos, N.:
285 Particle water and pH in the eastern Mediterranean: source variability and implications for nutrient availability, Atmos. Chem. Phys., 16, 4579–4591, https://doi.org/10.5194/acp-16-4579-2016, 2016.

Boyce, S. D., and Hoffmann, M. R.: Kinetics and mechanism of the formation of hydroxymethanesulfonic acid at low pH, J. Phys. Chem., 88, 4740–4746, https://doi.org/10.1021/j150664a059, 1984.

Cao, C., Jiang, W. J., Wang, B. Y., Fang, J. H., Lang, J. D., Tian, G., Jiang, J. K., and Zhu, T. F.: Inhalable Microorganisms in

290   Beijing's $PM_{2.5}$ and PM_{10} Pollutants during a Severe Smog Event, Environ. Sci. Technol., 48, 1499–1507, https://doi.org/10.1021/es4048472, 2014.

Chen, W. T., Shao, M., Lu, S. H., Wang, M., Zeng, L. M., Yuan, B., and Liu, Y.: Understanding primary and secondary sources of ambient carbonyl compounds in Beijing using the PMF model, Atmos. Chem. Phys., 14, 3047–3062, https://doi.org/10.5194/acp-14-3047-2014, 2014.

295   Chen, Y., Xu, L., Humphry, T., Hettiyadura, A. P. S., Ovadnevaite, J., Huang, S., Poulain, L., Schroder, J. C., Campuzano-Jost, P., Jimenez, J. L., Herrmann, H., O'Dowd, C., Stone, E. A., and Ng, N. L.: Response of the Aerodyne Aerosol Mass Spectrometer to Inorganic Sulfates and Organosulfur Compounds: Applications in Field and Laboratory Measurements, Environ. Sci. Technol., 53, 5176–5186, https://doi.org/10.1021/acs.est.9b00884, 2019.

Cheng, J., Su, J., Cui, T., Li, X., Dong, X., Sun, F., Yang, Y., Tong, D., Zheng, Y., Li, Y., Li, J., Zhang, Q., and He, K.: Dominant
300   role of emission reduction in $PM_{2.5}$ air quality improvement in Beijing during 2013–2017: a model-based decomposition analysis, Atmos. Chem. Phys., 19, 6125–6146, https://doi.org/10.5194/acp-19-6125-2019, 2019.

Cheng, Y. F., Zheng, G. J., Wei, C., Mu, Q., Zheng, B., Wang, Z. B., Gao, M., Zhang, Q., He, K. B., Carmichael, G., Poschl, U., and Su, H.: Reactive nitrogen chemistry in aerosol water as a source of sulfate during haze events in China, Sci. Adv., 2, e1601530, https://doi.org/10.1126/sciadv.1601530, 2016.

305   Dabek-Zlotorzynska, E., Piechowski, M., Keppel-Jones, K., and Aranda-Rodriguez, R.: Determination of hydroxymethanesulfonic acid in environmental samples by capillary electrophoresis, J. Sep. Sci., 25, 1123–1128, https://doi.org/10.1002/1615-9314(20021101)25:15/17<1123::aid-jssc1123>3.0.co;2-3, 2002.

Dall'Osto, M., Harrison, R. M., Coe, H., and Williams, P.: Real-time secondary aerosol formation during a fog event in London, Atmos. Chem. Phys., 9, 2459–2469, https://doi.org/10.5194/acp-9-2459-2009, 2009.

310   Dasgupta, P. K., Decesare, K., and Ullrey, J. C.: Determination of atmospheric sulfur-dioxide without tetrachloromercurate (II) and the mechanism of the schiff reaction, Anal. Chem., 52, 1912–1922, https://doi.org/10.1021/ac50062a031, 1980.

Dasgupta, P. K.: On the ion chromatographic determination of S(IV), Atmos. Environ., 16, 1265–1268, https://doi.org/10.1016/0004-6981(82)90217-7, 1982.

De Smedt, I., Stavrakou, T., Hendrick, F., Danckaert, T., Vlemmix, T., Pinardi, G., Theys, N., Lerot, C., Gielen, C., Vigouroux,
315   C., Hermans, C., Fayt, C., Veefkind, P., Müller, J. F., and Van Roozendael, M.: Diurnal, seasonal and long-term variations of global formaldehyde columns inferred from combined OMI and GOME-2 observations, Atmos. Chem. Phys., 15, 12519–12545, https://doi.org/10.5194/acp-15-12519-2015, 2015.

Deister, U., Neeb, R., Helas, G., and Warneck, P.: Temperature Dependence of the Equilibrium $CH_2(OH)_2 + HSO_3^- = CH_2(OH)SO_3^- + H_2O$ in Aqueous Solution, J. Phys. Chem., 90, 3213–3217, https://doi.org/10.1021/j100405a033, 1986.

320   Ding, J., Zhao, P., Su, J., Dong, Q., Du, X., and Zhang, Y.: Aerosol pH and its driving factors in Beijing, Atmos. Chem. Phys., 19, 7939–7954, https://doi.org/10.5194/acp-19-7939-2019, 2019.

Dixon, R. W., and Aasen, H.: Measurement of hydroxymethanesulfonate in atmospheric aerosols, Atmos. Environ., 33, 2023–2029, https://doi.org/10.1016/s1352-2310(98)00416-6, 1999.

Dovrou, E., Lim, C. Y., Canagaratna, M. R., Kroll, J. H., Worsnop, D. R., and Keutsch, F. N.: Measurement techniques for identifying and quantifying hydroxymethanesulfonate (HMS) in an aqueous matrix and particulate matter using aerosol mass spectrometry and ion chromatography, Atmos. Meas. Tech., 12, 5303–5315, https://doi.org/10.5194/amt-12-5303-2019, 2019.

Fountoukis, C., and Nenes, A.: ISORROPIA II: a computationally efficient thermodynamic equilibrium model for K^+-Ca^{2+}-Mg^{2+}-NH_4^+-Na^+-SO_4^{2-}-NO_3^--Cl^--H_2O aerosols, Atmos. Chem. Phys., 7, 4639–4659, https://doi.org/10.5194/acp-7-4639-2007, 2007.

Furutani, H., Jung, J., Miura, K., Takami, A., Kato, S., Kajii, Y., and Uematsu, M.: Single-particle chemical characterization and source apportionment of iron-containing atmospheric aerosols in Asian outflow, J. Geophys. Res. Atmos., 116, D18204, https://doi.org/10.1029/2011jd015867, 2011.

Ge, B., Xu, X., Ma, Z., Pan, X., Wang, Z., Lin, W., Ouyang, B., Xu, D., Lee, J., Zheng, M., Ji, D., Sun, Y., Dong, H., Squires, F. A., Fu, Q., and Wang, Z.: Role of Ammonia on the Feedback Between AWC and Inorganic Aerosol Formation During Heavy Pollution in the North China Plain, Earth and Space Science, 6, 1675–1693. https://doi.org/10.1029/2019ea000799, 2019.

Hak, C., Pundt, I., Trick, S., Kern, C., Platt, U., Dommen, J., Ordonez, C., Prevot, A. S. H., Junkermann, W., Astorga-Llorens, C., Larsen, B. R., Mellqvist, J., Strandberg, A., Yu, Y., Galle, B., Kleffmann, J., Lorzer, J. C., Braathen, G. O., and Volkamer, R.: Intercomparison of four different in-situ techniques for ambient formaldehyde measurements in urban air, Atmos. Chem. Phys., 5, 2881–2900, https://doi.org/10.5194/acp-5-2881-2005, 2005.

Hatch, L. E., Creamean, J. M., Ault, A. P., Surratt, J. D., Chan, M. N., Seinfeld, J. H., Edgerton, E. S., Su, Y. X., and Prather, K. A.: Measurements of Isoprene-Derived Organosulfates in Ambient Aerosols by Aerosol Time-of-Flight Mass Spectrometry - Part 1: Single Particle Atmospheric Observations in Atlanta, Environ. Sci. Technol., 45, 5105–5111, https://doi.org/10.1021/es103944a, 2011.

Hennigan, C. J., Izumi, J., Sullivan, A. P., Weber, R. J., and Nenes, A.: A critical evaluation of proxy methods used to estimate the acidity of atmospheric particles, Atmos. Chem. Phys., 15, 2775–2790, https://doi.org/10.5194/acp-15-2775-2015, 2015.

Hoigne, J., Bader, H., Haag, W. R., and Staehelin, J.: Rate constants of reactions of ozone with organic and inorganic-compounds in water .3. inorganic-compounds and radicals, Water Res., 19, 993–1004, https://doi.org/10.1016/0043-1354(85)90368-9, 1985.

Hu, J. L., Wang, P., Ying, Q., Zhang, H. L., Chen, J. J., Ge, X. L., Li, X. H., Jiang, J. K., Wang, S. X., Zhang, J., Zhao, Y., and Zhang, Y. Y.: Modeling biogenic and anthropogenic secondary organic aerosol in China, Atmos. Chem. Phys., 17, 77–92, https://doi.org/10.5194/acp-17-77-2017, 2017.

Huang, R. J., Zhang, Y., Bozzetti, C., Ho, K. F., Cao, J. J., Han, Y., Daellenbach, K. R., Slowik, J. G., Platt, S. M., Canonaco, F., Zotter, P., Wolf, R., Pieber, S. M., Bruns, E. A., Crippa1, M., Ciarelli, G., Piazzalunga, A., Schwikowski, M., Abbaszade, G., Schnelle-Kreis, J., Zimmermann, R., An, Z., Szidat, S., Baltensperger, U., Haddad, I. E., and Prévôt, A. S. H.: High secondary aerosol contribution to particulate pollution during haze events in China, Nature, 514, 218–222, https://doi.org/10.1038/nature13774, 2014.

Kok, G. L., Gitlin, S. N., and Lazrus, A. L.: Kinetics of the formation and decomposition of hydroxymethanesulfonate, J.

Geophys. Res. Atmos., 91, 2801–2804, https://doi.org/10.1029/JD091iD02p02801, 1986.

Lagrange, J., Wenger, G., and Lagrange, P.: Kinetic study of HMSA formation and decomposition: Tropospheric relevance, J.
360 Chim. Phys. Phys.- Chim. Biol., 96, 610–633, https://doi.org/10.1051/jcp:1999161, 1999.

Lee, S. H.: Nitrate and oxidized organic ions in single particle mass spectra during the 1999 Atlanta Supersite Project, J. Geophys. Res., 108, D78417, https://doi.org/10.1029/2001jd001455, 2003.

Lelieveld, J., Evans, J. S., Fnais, M., Giannadaki, D., and Pozzer, A.: The contribution of outdoor air pollution sources to premature mortality on a global scale, Nature, 525, 367–371, https://doi.org/10.1038/nature15371, 2015.

365 Li, C., McLinden, C., Fioletov, V., Krotkov, N., Carn, S., Joiner, J., Streets, D., He, H., Ren, X., Li, Z., and Dickerson, R. R.: India Is Overtaking China as the World's Largest Emitter of Anthropogenic Sulfur Dioxide, Sci. Rep., 7, 14304, https://doi.org/10.1038/s41598-017-14639-8, 2017.

Li, H., Cheng, J., Zhang, Q., Zheng, B., Zhang, Y., Zheng, G., and He, K.: Rapid transition in winter aerosol composition in Beijing from 2014 to 2017: response to clean air actions, Atmos. Chem. Phys., 19, 11485–11499, https://doi.org/10.5194/acp-
370 19-11485-2019, 2019a.

Li, M., Zhang, Q., Zheng, B., Tong, D., Lei, Y., Liu, F., Hong, C., Kang, S., Yan, L., Zhang, Y., Bo, Y., Su, H., Cheng, Y., and He, K.: Persistent growth of anthropogenic non-methane volatile organic compound (NMVOC) emissions in China during 1990-2017: drivers, speciation and ozone formation potential, Atmos. Chem. Phys., 19, 8897–8913, https://doi.org/10.5194/acp-2019-125, 2019b.

375 Liu, M., Song, Y., Zhou, T., Xu, Z., Yan, C., Zheng, M., Wu, Z., Hu, M., Wu, Y., and Zhu, T.: Fine particle pH during severe haze episodes in northern China, Geophys. Res. Lett., 44, 5213–5221, https://doi.org/10.1002/2017gl073210, 2017a.

Liu, Y., Wu, Z., Wang, Y., Xiao, Y., Gu, F., Zheng, J., Tan, T., Shang, D., Wu, Y., Zeng, L., Hu, M., Bateman, A. P., and Martin, S. T.: Submicrometer Particles Are in the Liquid State during Heavy Haze Episodes in the Urban Atmosphere of Beijing, China, Environ. Sci. Tech. Lett., 4, 427–432, https://doi.org/10.1021/acs.estlett.7b00352, 2017b.

380 Moch, J. M., Dovrou, E., Mickley, L. J., Keutsch, F. N., Cheng, Y., Jacob, D. J., Jiang, J., Li, M., Munger, J. W., Qiao, X., and Zhang, Q.: Contribution of hydroxymethane sulfonate to ambient particulate matter: A potential explanation for high particulate sulfur during severe winter haze in Beijing, Geophys. Res. Lett., 45, 11969–11979, https://doi.org/10.1029/2018gl079309, 2018.

Munger, J. W., Tiller, C., and Hoffmann, M. R.: Identification of hydroxymethanesulfonate in fog water, Science, 231, 247–
385 249, https://doi.org/10.1126/science.231.4735.247, 1986.

Neubauer, K. R., Johnston, M. V., and Wexler, A. S.: On-line analysis of aqueous aerosols by laser desorption ionization, Int. J. Mass Spectrom. Ion Processes, 163, 29–37, https://doi.org/10.1016/s0168-1176(96)04534-x, 1997.

Niu, H., Mo, Z. W., Shao, M., Lu, S. H., and Xie, S. D.: Screening the emission sources of volatile organic compounds (VOCs) in China by multi-effects evaluation, Front. Environ. Sci. Eng., 10, 11, https://doi.org/10.1007/s11783-016-0828-z, 2016.

390 Pandis, S. N., and Seinfeld, J. H.: Sensitivity analysis of a chemical mechanism for aqueous-phase atmospheric chemistry, J. Geophys. Res. Atmos., 94, 1105–1126, https://doi.org/10.1029/JD094iD01p01105, 1989.

Rao, X., and Collett, J. L.: Behavior of S(IV) and formaldehyde in a chemically heterogeneous cloud, Environ. Sci. Technol., 29, 1023–1031, https://doi.org/10.1021/es00004a024, 1995.

Rao, Z. H., Chen, Z. M., Liang, H., Huang, L. B., and Huang, D.: Carbonyl compounds over urban Beijing: Concentrations on haze and non-haze days and effects on radical chemistry, Atmos. Environ., 124, 207–216, https://doi.org/10.1016/j.atmosenv.2015.06.050, 2016.

Sander, R.: Compilation of Henry's law constants (version 4.0) for water as solvent, Atmos. Chem. Phys., 15, 4399–4981, https://doi.org/10.5194/acp-15-4399-2015, 2015.

Scheinhardt, S., van Pinxteren, D., Muller, K., Spindler, G., and Herrmann, H.: Hydroxymethanesulfonic acid in size-segregated aerosol particles at nine sites in Germany, Atmos. Chem. Phys., 14, 4531–4538, https://doi.org/10.5194/acp-14-4531-2014, 2014.

Sheng, J., Zhao, D., Ding, D., Li, X., Huang, M., Gao, Y., Quan, J., and Zhang, Q.: Characterizing the level, photochemical reactivity, emission, and source contribution of the volatile organic compounds based on PTR-TOF-MS during winter haze period in Beijing, China, Atmos. Res., 212, 54–63, https://doi.org/10.1016/j.atmosres.2018.05.005, 2018.

Song, S., Gao, M., Xu, W., Sun, Y., Worsnop, D. R., Jayne, J. T., Zhang, Y., Zhu, L., Li, M., Zhou, Z., Cheng, C., Lv, Y., Wang, Y., Peng, W., Xu, X., Lin, N., Wang, Y., Wang, S., Munger, J. W., Jacob, D. J., and McElroy, M. B.: Possible heterogeneous chemistry of hydroxymethanesulfonate (HMS) in northern China winter haze, Atmos. Chem. Phys., 19, 1357–1371, https://doi.org/10.5194/acp-19-1357-2019, 2019.

Song, S. J., Gao, M., Xu, W. Q., Shao, J. Y., Shi, G. L., Wang, S. X., Wang, Y. X., Sun, Y. L., and McElroy, M. B.: Fine-particle pH for Beijing winter haze as inferred from different thermodynamic equilibrium models, Atmos. Chem. Phys., 18, 7423–7438, https://doi.org/10.5194/acp-18-7423-2018, 2018.

Suzuki, Y., Kawakami, M., and Akasaka, K.: H-1 NMR application for characterizing water-soluble organic compounds in urban atmospheric particles, Environ. Sci. Technol., 35, 2656–2664, https://doi.org/10.1021/es001861a, 2001.

Tan, Z. F., Rohrer, F., Lu, K. D., Ma, X. F., Bohn, B., Broch, S., Dong, H. B., Fuchs, H., Gkatzelis, G. I., Hofzumahaus, A., Holland, F., Li, X., Liu, Y., Liu, Y. H., Novelli, A., Shao, M., Wang, H. C., Wu, Y. S., Zeng, L. M., Hu, M., Kiendler-Scharr, A., Wahner, A., and Zhang, Y. H.: Wintertime photochemistry in Beijing: observations of ROx radical concentrations in the North China Plain during the BEST-ONE campaign, Atmos. Chem. Phys., 18, 12391–12411, https://doi.org/10.5194/acp-18-12391-2018, 2018.

Wang, G. H., Zhang, R. Y., Gomez, M. E., Yang, L. X., Zamora, M. L., Hu, M., Lin, Y., Peng, J. F., Guo, S., Meng, J. J., Li, J. J., Cheng, C. L., Hu, T. F., Ren, Y. Q., Wang, Y. S., Gao, J., Cao, J. J., An, Z. S., Zhou, W. J., Li, G. H., Wang, J. Y., Tian, P. F., Marrero-Ortiz, W., Secrest, J., Du, Z. F., Zheng, J., Shang, D. J., Zeng, L. M., Shao, M., Wang, W. G., Huang, Y., Wang, Y., Zhu, Y. J., Li, Y. X., Hu, J. X., Pan, B., Cai, L., Cheng, Y. T., Ji, Y. M., Zhang, F., Rosenfeld, D., Liss, P. S., Duce, R. A., Kolb, C. E., and Molina, M. J.: Persistent sulfate formation from London Fog to Chinese haze, Proc. Natl. Acad. Sci. U. S. A., 113, 13630–13635, https://doi.org/10.1073/pnas.1616540113, 2016.

Wang, Y., Zhang, Q., Jiang, J., Zhou, W., Wang, B., He, K., Duan, F., Zhang, Q., Philip, S., and Xie, Y.: Enhanced sulfate

formation during China's severe winter haze episode in January 2013 missing from current models, J. Geophys. Res. Atmos., 119, 10425–10440, https://doi.org/10.1002/2013JD021426, 2014.

Weber, R. J., Guo, H., Russell, A. G., and Nenes, A.: High aerosol acidity despite declining atmospheric sulfate concentrations over the past 15 years, Nat. Geosci., 9, 282–285, https://doi.org/10.1038/ngeo2665, 2016.

430   Whiteaker, J. R., and Prather, K. A.: Hydroxymethanesulfonate as a tracer for fog processing of individual aerosol particles, Atmos. Environ., 37, 1033–1043, https://doi.org/10.1016/s1352-2310(02)01029-4, 2003.

Xing, L., Fu, T. M., Cao, J. J., Lee, S. C., Wang, G. H., Ho, K. F., Cheng, M. C., You, C. F., and Wang, T. J.: Seasonal and spatial variability of the OM/OC mass ratios and high regional correlation between oxalic acid and zinc in Chinese urban organic aerosols, Atmos. Chem. Phys., 13, 4307–4318, https://doi.org/10.5194/acp-13-4307-2013, 2013.

435   Xu, L. L., Duan, F. K., He, K. B., Ma, Y. L., Zhu, L. D., Zheng, Y. X., Huang, T., Kimoto, T., Ma, T., Li, H., Ye, S. Q., Yang, S., Sun, Z. L., and Xu, B. Y.: Characteristics of the secondary water-soluble ions in a typical autumn haze in Beijing, Environ. Pollut., 227, 296–305, https://doi.org/10.1016/j.envpol.2017.04.076, 2017.

Yang, W., Li, J., Wang, M., Sun, Y., and Wang, Z.: A Case Study of Investigating Secondary Organic Aerosol Formation Pathways in Beijing using an Observation-based SOA Box Model, Aerosol Air Qual. Res., 18, 1606–1616,
440   https://doi.org/10.4209/aaqr.2017.10.0415, 2018.

Ye, C., Liu, P., Ma, Z., Xue, C., Zhang, C., Zhang, Y., Liu, J., Liu, C., Sun, X., and Mu, Y.: High H_2O_2 Concentrations Observed during Haze Periods during the Winter in Beijing: Importance of H_2O_2 Oxidation in Sulfate Formation, Environ. Sci. Tech. Lett., 5, 757–763, https://doi.org/10.1021/acs.estlett.8b00579, 2018.

Zhang, X., He, S. Z., Chen, Z. M., Zhao, Y., and Hua, W.: Methyl hydroperoxide (CH_3OOH) in urban, suburban and rural
445   atmosphere: ambient concentration, budget, and contribution to the atmospheric oxidizing capacity, Atmos. Chem. Phys., 12, 8951–8962, https://doi.org/10.5194/acp-12-8951-2012, 2012.

Zhang, Y. J., Cai, J., Wang, S. X., He, K. B., and Zheng, M.: Review of receptor-based source apportionment research of fine particulate matter and its challenges in China, Sci. Total Environ., 586, 917–929, https://doi.org/10.1016/j.scitotenv.2017.02.071, 2017.

450   Zhao, B., Wang, S., Donahue, N. M., Jathar, S. H., Huang, X., Wu, W., Hao, J., and Robinson, A. L.: Quantifying the effect of organic aerosol aging and intermediate-volatility emissions on regional-scale aerosol pollution in China, Sci. Rep., 6, 28815, https://doi.org/10.1038/srep28815, 2016.

Zheng, B., Zhang, Q., Zhang, Y., He, K. B., Wang, K., Zheng, G. J., Duan, F. K., Ma, Y. L., and Kimoto, T.: Heterogeneous chemistry: a mechanism missing in current models to explain secondary inorganic aerosol formation during the January 2013
455   haze episode in North China, Atmos. Chem. Phys., 15, 2031–2049, https://doi.org/10.5194/acp-15-2031-2015, 2015a.

Zheng, B., Tong, D., Li, M., Liu, F., Hong, C., Geng, G., Li, H., Li, X., Peng, L., Qi, J., Yan, L., Zhang, Y., Zhao, H., Zheng, Y., He, K., and Zhang, Q.: Trends in China's anthropogenic emissions since 2010 as the consequence of clean air actions, Atmos. Chem. Phys., 18, 14095–14111, https://doi.org/10.5194/acp-18-14095-2018, 2018.

Zheng, G. J., Duan, F. K., Su, H., Ma, Y. L., Cheng, Y., Zheng, B., Zhang, Q., Huang, T., Kimoto, T., Chang, D., Pöschl, U.,

460   Cheng, Y. F., and He, K. B.: Exploring the severe winter haze in Beijing: the impact of synoptic weather, regional transport and heterogeneous reactions, Atmos. Chem. Phys., 15, 2969–2983, https://doi.org/10.5194/acp-15-2969-2015, 2015b.
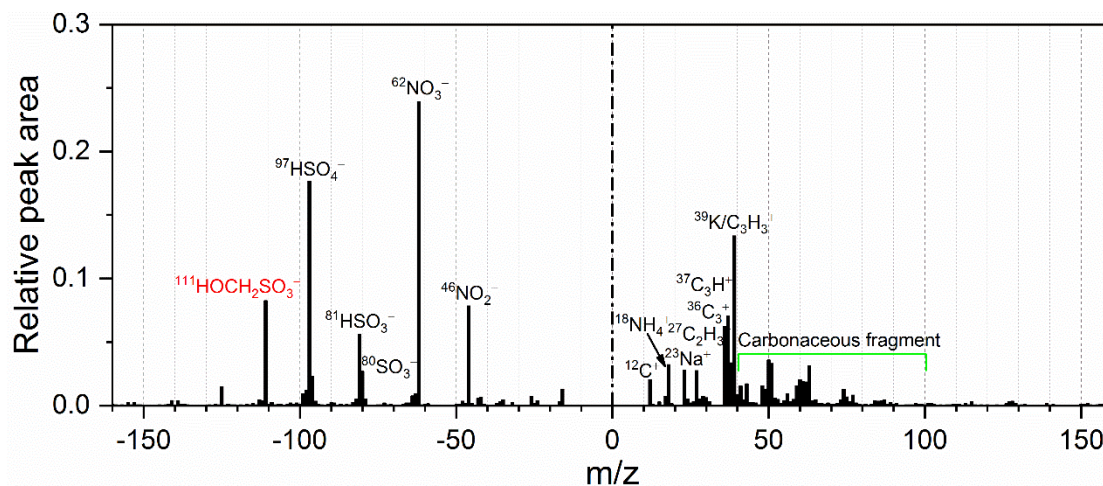
Figure 1. Presence of HMS in single particle mass spectra during winter in Beijing. The peak at *m/z* 111 in the negative ion mode is attributed to HMS (HOCH$_2$SO$_3^-$). The peaks at *m/z* 80 (SO$_3^-$), 81 (HSO$_3^-$), 97 (HSO$_4^-$), 46 (NO$_2^-$), and 62 (NO$_3^-$) are also common in the negative ion spectrum, indicating the presence of sulfur species and nitrate. In the positive mass spectra, inorganic ions (*m/z* 18 NH$_4^+$, 23 Na$^+$, and 39 K$^+$), elemental carbon (*m/z* 12 C$^+$, 36 C$_3^+$, and 48 C$_4^+$), and organic carbon (*m/z* 27 C$_2$H$_3^+$, 37 C$_3$H$^+$, 39 C$_3$H$_3^+$, and 43 C$_2$H$_3$O$^+$) are present.
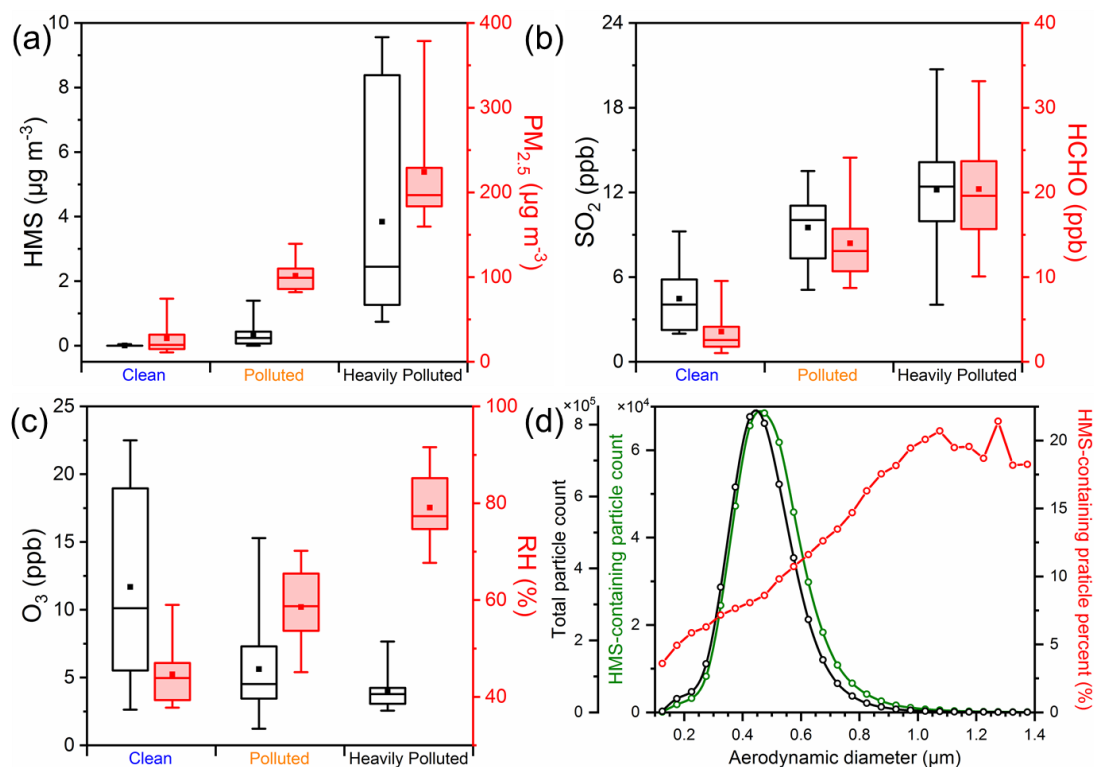
Figure 2. Evolution of HMS in Beijing winter of 2015. **(a-c)** Concentrations of HMS, PM$_{2.5}$, SO$_2$, HCHO, and O$_3$, and RH at

470 different pollution levels from 26 November 2015 to 8 January 2016. In the box-whisker plots, the whiskers, boxes, and points indicate the 95th, 75th, 50th, 25th, 5th percentiles and mean values, respectively. **(d)** Size distribution of HMS-containing particles from 21 December 2015 to 8 January 2016.
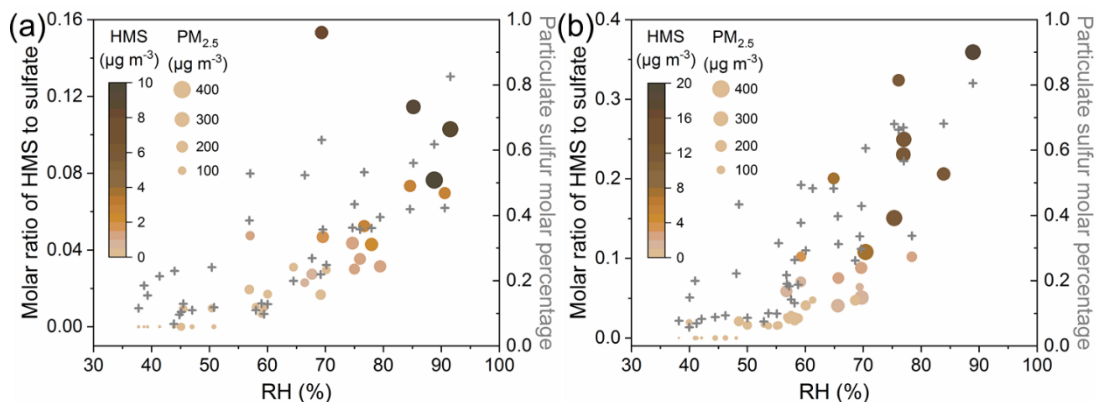
Figure 3. Evolution of sulfur distribution with the increase of RH in the winter of **(a)** 2015 and **(b)** 2016. The solid circles
475 represent the molar ratio of HMS to sulfate, with colored by the HMS concentrations and sized by the PM$_{2.5}$ concentrations. The gray crosses represent the particulate sulfur molar percentage. Particulate sulfur molar percentage =

$$\frac{n(SO_4^{2-})+n(HMS)}{n(SO_4^{2-})+n(HMS)+n(SO_2)}.$$
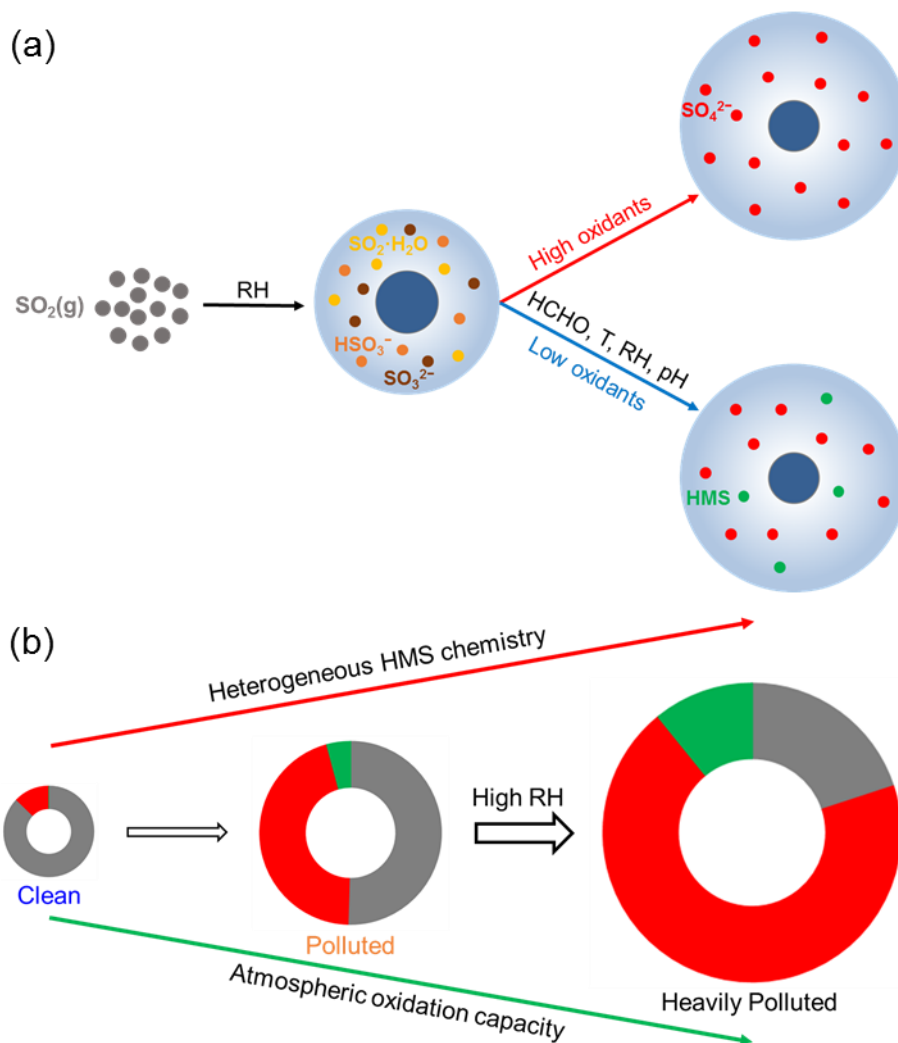
Figure 4. Schematic of the heterogeneous sulfur chemistry. **(a)** Oxidation and addition reaction pathways of dissolved SO_2 in aerosol water under different atmospheric conditions. **(b)** Evolution of sulfur-containing species during winter haze deterioration in the NCP. With the increase of RH and decrease of atmospheric oxidation capacity under NCP winter haze, the atmospheric sulfur distribution shifts toward the particle phase and more particulate sulfur exists in the form of HMS. The gray, red, and green colors represent SO_2, SO_4^{2-} and HMS, respectively.